

Influence of Biophysical Parameters on Maintaining the Mesenchymal Stem Cell Phenotype

Junmin Lee, Amr A. Abdeen, Alex S. Kim, and Kristopher A. Kilian*

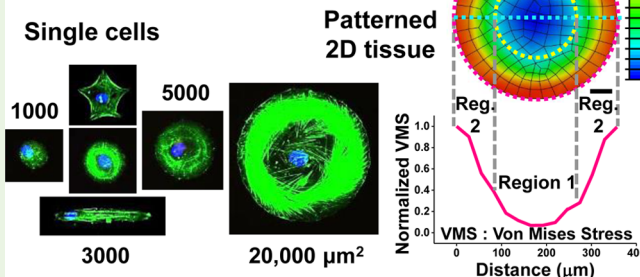
Department of Materials Science and Engineering, Micro and Nanotechnology Laboratory, University of Illinois at Urbana–Champaign, Urbana, Illinois 61801, United States

Supporting Information

ABSTRACT: The maintenance of the mesenchymal stem cell (MSC) phenotype *in vivo* is influenced by the precise orchestration of biochemical and biophysical signals in the stem cell “niche”. However, when MSCs are removed from the body and expanded *in vitro*, there is a loss of multipotency. Here, we employ micropatterned hydrogels to explore how biophysical cues influence the retention of MSC multipotency marker expression. At the single-cell level, soft substrates and patterns that restrict spreading and cytoskeletal tension help maintain the expression of MSC markers. When MSCs are patterned in multicellular geometries, both high cell density and regions of low tension within the pattern are shown to assist the maintenance of multipotency. Combining experiment and simulation along with cytoskeleton disrupting agents reveals spatial patterns of cytoskeletal tension in multicellular architectures that guides the expression of markers associated with MSC multipotency. These findings uncover a relationship between multiple biophysical parameters in maintaining the MSC phenotype, which may shed light on the structure of the MSC “niche” and prove useful in guiding the selection of *in vitro* expansion materials for regenerative therapies.

KEYWORDS: mesenchymal stem cells, multipotency, hydrogels, matrix elasticity, cell shape

Maintenance of multipotency (soft & stiff hydrogels)



1. INTRODUCTION

The stem cell niche is a specialized microenvironment that supports quiescence, self-renewal to maintain a stable stem cell population, and proliferation to replenish tissue-specific cell types.^{1–3} Mesenchymal stem cells (MSCs), defined as unspecialized precursor cells isolated from bone marrow and other adult tissues, possess two fundamental characteristics: their ability to self-renew and their ability to differentiate into a variety of lineages including osteoblasts, adipocytes, chondrocytes, and stromal support cells under appropriate stimuli.^{4–6} When proliferating in culture, MSCs are devoid of hematopoietic and endothelial markers (e.g., CD34, CD45) and express distinct level of CD90, CD105 (Endoglin), and Stro-1.⁷ These MSC-positive markers serve to classify the degree of “stemness” for *in vitro* culture with a significant decrease during differentiation.⁸ The biophysical and biochemical properties of the extracellular matrix (ECM) play a significant role in regulating stem cell migration, proliferation and differentiation.^{9–15} A major research effort has gone into devising *in vitro* engineered ECMs to unravel the complex interplay of factors that control stem cell differentiation.^{16–20} However, the role that ECM properties play in guiding the multipotent phenotype and self-renewal has received significantly less attention. Gilbert et al. demonstrated skeletal muscle stem cell self-renewal was heavily influenced by the stiffness of the surrounding material,²¹ and Winer et al. showed how soft

substrates promote MSC quiescence; MSCs on very soft substrates (~ 0.25 kPa) that mimic the stiffness of bone marrow are quiescent but retain the ability to differentiate when exposed to induction media.¹⁴ Recently, Skardal et al. reported how soft substrates promote the expression of MSC surface markers in amniotic fluid-derived stem cells.²² These reports suggest that the mechanical properties of the cell culture substrate may influence MSC multipotency.

Topography and tissue geometry also guide cellular processes *in vivo*. Oh et al. and Park et al. showed that the nanoscale architecture of titanium nanotubes can influence MSC differentiation.^{23,24} McMurray et al. demonstrated how the ordered arrangement of the substrate’s nanotopography will enable long-term maintenance of the MSC phenotype.²⁵ Micropatterning tools that manipulate the size and shape of *in vitro* cellular assemblies have also proved useful in deconstructing the mechanochemical signals that regulate lineage specific gene expression.^{26–29} For example, cell survival was shown to be linked to cell size via cytoskeletal tension based signaling pathways such as RhoA-ROCK.²⁶ In addition, the shape of single MSCs,^{12,27} and geometric cues at the perimeter of multicellular architectures,^{30,31} will guide differ-

Received: September 10, 2014

Accepted: March 2, 2015

Published: March 2, 2015

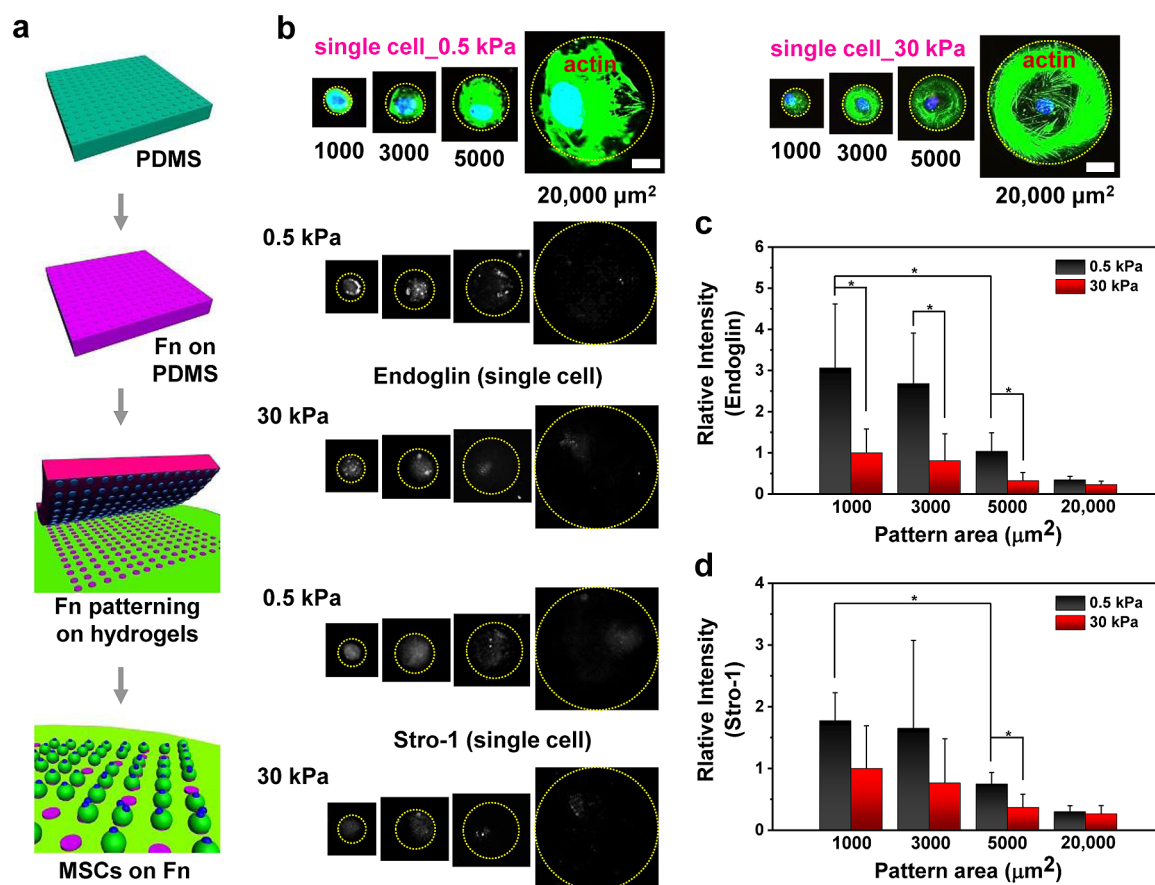


Figure 1. Combinations of stiffness and cell size differentially modulate MSC marker expression. (a) Schematic showing the process used to pattern cells on polyacrylamide (PA). (b) Representative immunofluorescence microscope images of MSCs stained for Endoglin and Stro-1 cultured on soft (0.5 kPa) and stiff (30 kPa) PA hydrogels for 10 days (1000–20,000 μm^2). Scale bar: 40 μm . Quantitation of (c) Endoglin and (d) Stro-1 markers for patterned cells cultured on soft and stiff substrates for 10 days. ($N = 4$). (* $P < 0.05$, one-way ANOVA).

entiation through control of cytoskeletal tension. For example, cells on the perimeter of concave regions, which promote higher mechanical stress, prefer to differentiate to the osteogenic lineage.³⁰ In contrast, MSCs at the interior of patterns, or in convex regions with a low degree of stress, tend to differentiate into adipocytes.

Recently, we showed how confining MSCs into small islands can restrict inappropriate lineage specification and enhance the expression of MSC markers compared to cells cultured on plastic.³² In the present report we explore the role of substrate stiffness—alone and when combined with geometric cues—in modulating the MSC multipotent phenotype. Polyacrylamide hydrogels are fabricated across a range of mechanical properties and microcontact printed with matrix proteins in shapes that accommodate single cells to several hundreds of cells. Immunofluorescence characterization of MSC markers, coupled with computer simulations and pharmacological inhibitors of actomyosin contractility, reveals spatial control of multipotency directed by the stiffness of the underlying substrate and cellular organization.

2. MATERIALS AND METHODS

2.1. Materials. Human MSCs were purchased from Lonza. The MSCs were harvested and cultured from normal bone marrow. Cells were tested for the ability of differentiation and the results showed that osteogenic, chondrogenic, or adipogenic lineage commitments are possible. Cells were positive for CD105, CD166, CD29, and CD44 and negative for CD14, CD34, and CD45 by flow cytometry ([\[www.lonza.com\]\(http://www.lonza.com\)\). Cell culture media and reagents were purchased from Gibco. BrdU reagent was purchased from Invitrogen. Mouse anti-Stro-1 antibody was purchased from R&D Systems \(MAB1038\), rabbit anti-Endoglin was purchased from Sigma \(E7534\), and rabbit anti-BrdU was purchased from Sigma \(B2531\). Tetramethylrhodamine-conjugated antirabbit IgG antibody, Alexa Fluor 647-conjugated antimouse IgG antibody, Alexa Fluor 555-conjugated antirabbit IgG antibody, Alexa488-phalloidin and 4,6-diamidino-2-phenylindole \(DAPI\) were purchased from Invitrogen. 12-well tissue culture plastic ware and glass coverslips \(18 mm circular\) for surface preparation were purchased from Fisher Scientific. Other laboratory chemicals and reagents were purchased from Sigma-Aldrich.](http://</p>
</div>
<div data-bbox=)

2.2. Surface Preparation. Polyacrylamide gels were fabricated on a glass coverslip (18 mm) as reported previously.³³ Hydrogels of varying stiffness were made by mixing varying amounts of acrylamide and bis-acrylamide to get the desired stiffness. To initiate the reaction, 0.1% ammonium persulfate (APS) and 0.1% of tetramethylethylenediamine (TEMED) were employed. The amino-silanized coverslips (3-aminopropyltriethoxysilane 3 min and glutaraldehyde 30 min) were added with the treated side down onto hydrophobically treated glass slides with 20 μl of the gel mixture. After an appropriate polymerization time for each stiffness condition, the gel-coated coverslips were gently detached. Hydrazine hydrate (55%) was added for 2 h to convert amide groups in polyacrylamide to reactive hydrazide groups.³⁴ The gels were washed for an hour in 5% glacial acetic acid and for 1 h in distilled water. Polydimethylsiloxane (PDMS, Polysciences, Inc.) stamps were produced by conventional polymerization methods on silicon masters patterned with photoresist (SU-8, Micro-Chem), which were created using UV photolithography through a laser printed mask or unpatterned (flat) surfaces. After

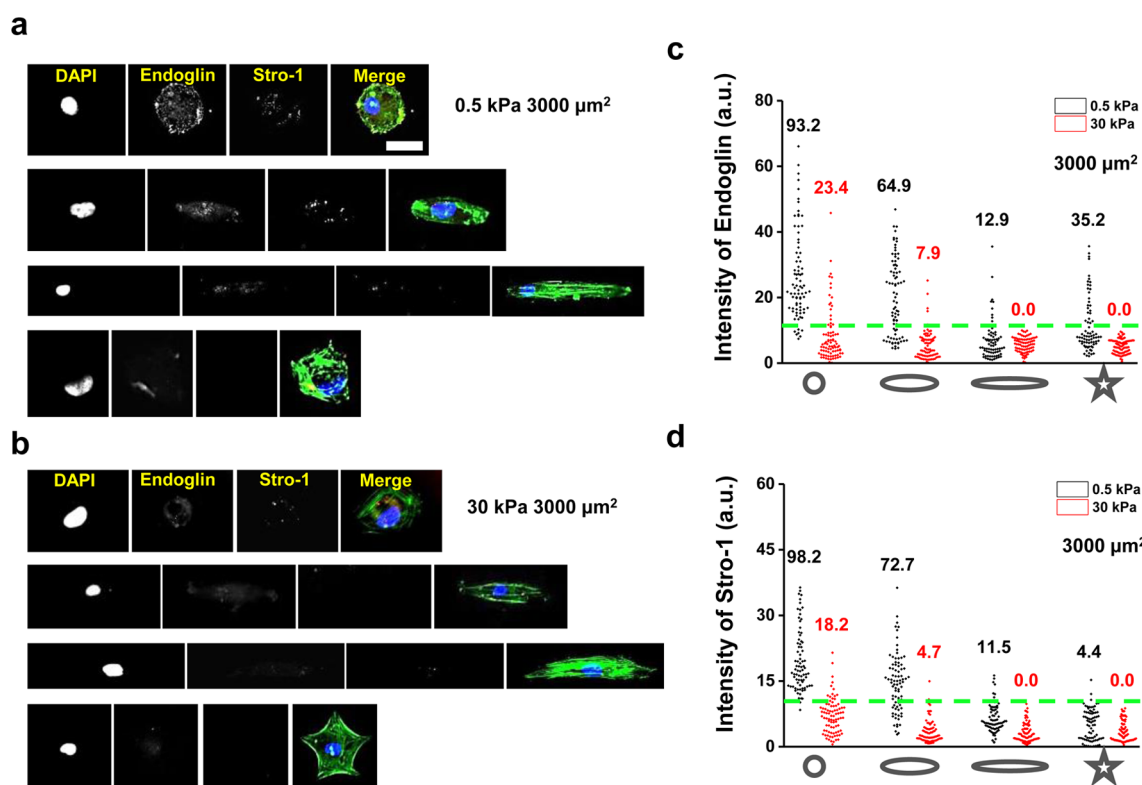


Figure 2. Combining geometric cues and matrix stiffness to study the maintenance of MSC multipotency. (a) Representative immunofluorescence microscope images of MSCs stained for Endoglin and Stro-1 cultured in various geometries (circle, ovals (4:1 and 8:1), and star) on (a) soft (0.5 kPa) and (b) stiff (30 kPa) substrates (Scale bar: 40 μm). Quantitation (%) of (c) Endoglin and (d) Stro-1 markers for patterned cells cultured on soft and stiff substrates for 10 days. The threshold (dashed line) was selected by comparing the highest and lowest marker intensities.

curing, the PDMS stamps were gently detached from the molds. Sodium periodate (~ 3.5 mg/mL, Sigma-aldrich) was employed to generate free aldehydes on matrix proteins. It was added to 25 $\mu\text{g}/\text{mL}$ of fibronectin in PBS for at least 45 min. The protein solution was pipetted onto patterned or flat (nonpatterned) stamps for 30 min. The protein solution on the surface of the stamp was dried with air and then the protein residues on stamps were transferred to the gel surfaces; free aldehydes in proteins were chemically conjugated with reactive hydrazide groups on the gels.

2.3. Cell Source and Culture. MSCs from bone marrow were thawed from cryopreservation (10% DMSO) and cultured in Dulbecco's modified eagle's medium (DMEM) low glucose (1 g/mL) media supplemented with 10% fetal bovine serum (MSC approved FBS; Invitrogen), and 1% penicillin/streptomycin (p/s). Media was changed every 3 or 4 days. Passage 4–7 MSCs were seeded on patterned and nonpatterned surfaces at a cell density of ~ 5000 cells/ cm^2 . MSCs were cultured for 10 days before analysis.

2.4. Immunocytochemistry. Cells on surfaces were fixed with 4% paraformaldehyde (Alfa Aesar) for 20 min, permeabilized in 0.1% Triton X-100 in PBS for 30 min and blocked with 1% bovine serum albumin (BSA) for 15 min. Primary antibody labeling was performed in 1% BSA in PBS for 2 h at room temperature (20 $^{\circ}\text{C}$) with mouse anti-Stro-1 and rabbit anti-Endoglin and anti-BrdU (1:200 dilution). Secondary antibody labeling was performed using the same procedure with Tetramethylrhodamine-conjugated antirabbit IgG antibody, Alexa Fluor 488-phalloidin (1:200 dilution), Alexa647-conjugated antimouse IgG antibody, and 4,6-diamidino-2-phenylindole (DAPI, 1:5000 dilution) for 20 min in a humid chamber (37 $^{\circ}\text{C}$). Immunofluorescence microscopy was conducted using a Zeiss Axiovert 200 M inverted research-grade microscope (Carl Zeiss, Inc.) or an LSM 700 (Carl Zeiss, Inc.) which is a four laser point scanning confocal with a single pinhole. Immunofluorescent images from the immunofluorescence microscopy or the LSM 700 were analyzed using ImageJ; the fluorescence intensity of single cells (over 20 cells) and multiple cells (over 20 patterns) for each condition were measured to compare

stemness marker expression. All results were confirmed at least three times. The relative intensity of the fluorescence was determined by comparing each intensity value to the average intensity of one condition. For Figure 1, average Endoglin and Stro-1 marker intensities of cells in 1000 μm^2 patterned stiff (30 kPa) substrates were selected. For Figure 2, average Endoglin and Stro-1 marker intensities of untreated cells were selected. The intensity value for single cells was obtained from cytoplasmic staining intensity minus backgrounds and for multiple cells total cell intensities (minus background) were obtained for each condition.

2.5. BrdU Staining. BrdU staining was conducted to check MSC proliferation as reported previously.³² Briefly, 1 h postseeding, nonadherent cells were aspirated and BrdU labeling reagent was added (1:100 (v/v)), and incubated for 24 h. Cultures were fixed in 70% ethanol for 30 min and then denatured with 2 M HCl for 30 min. Cultures were permeabilized with 0.1% Triton X-100 in PBS for 30 min and blocked with 1% BSA in PBS for 15 min and then incubated with mouse anti-BrdU primary antibody (1:200 dilution, 3 h at room temperature) followed by Alexa Fluor 647-conjugated antimouse IgG antibody (1:200 dilution, 20 min in a humid chamber (37 $^{\circ}\text{C}$)). Cell nuclei were stained with DAPI (1:5000 dilutions). Percent incorporation of BrdU was counted manually.

2.6. Modeling of Cell Monolayer. A finite-element model of contractile cell monolayers was constructed using ABAQUS FEA software as described before.³¹ Briefly, a model with the desired geometry was constructed consisting of 2 layers: an active 20 μm thickness top layer and a passive 5 μm bottom layer fixed at the bottom surface. The physical parameters used were those described previously.³¹ Contractility was introduced to the active layer by applying a 5K temperature drop to induce isotropic thermal strain. The von Mises stress at the bottom surface was reported. Convergence of results was confirmed by testing multiple mesh sizes and layer properties.

2.7. Inhibition Assays. Inhibitors were added to cell culture media at the following concentrations before and after cell seeding and with

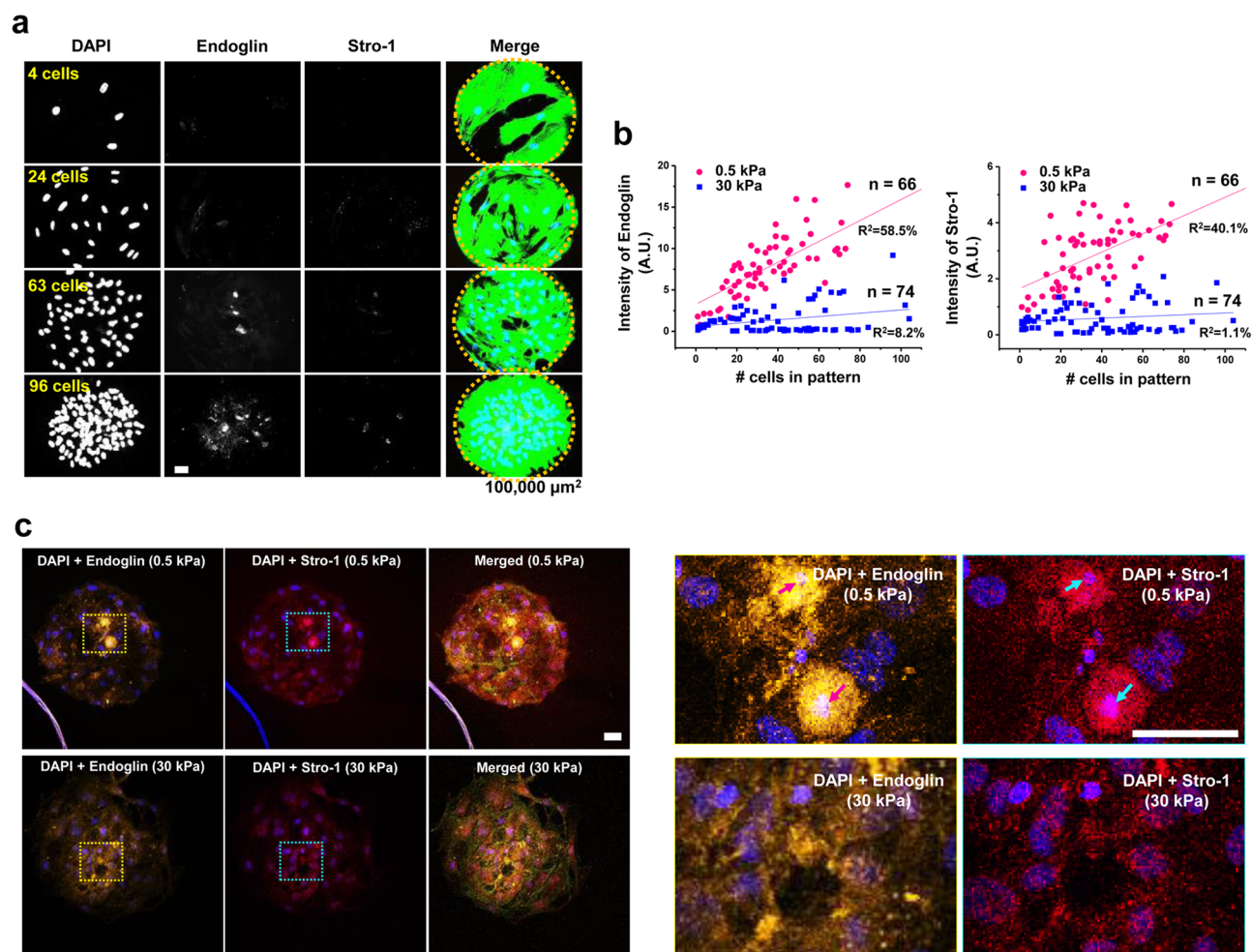


Figure 3. Cell density in multicellular patterns leads to different degrees of MSC marker expression. (a) Representative immunofluorescence microscope images of MSCs with different density in the same size patterns ($100\,000\ \mu\text{m}^2$). Plot of all measured immunofluorescence intensity data (Endoglin and Stro-1) versus a number of (b) MSCs (stem cells from bone marrow). (c) Representative laser scanning confocal microscope images of MSCs on soft (0.5 kPa) or stiff (30 kPa) substrates: MSC nuclei (blue), actin (cyan-green), Endoglin (yellow-orange), Stro-1 (red). Scale bar: 40 μm .

each media change: Blebbistatin (1 μM) and Y-27632 (2 μM) (Calbiochem).

2.8. Statistical Analysis. Error bars represent standard deviation and N value is the number of experimental replicates. For statistical analysis, we used one-way ANOVA for comparing multiple groups and two-tailed p -values from unpaired t test for comparing two groups, and values of $P < 0.05$ were considered statistically significant.

3. RESULTS

3.1. Hydrogel Fabrication and Patterning. To study the combined influence of substrate stiffness and cell shape on MSC phenotype, we used protein-conjugated polyacrylamide hydrogels. The procedure is schematically presented in Figure 1a. Soft (0.5 kPa) and stiff (30 kPa) hydrogels were prepared according to established methods.³³ Microcontact printing was employed to transfer oxidized fibronectin from polydimethylsiloxane (PDMS) stamps—patterned using photolithography to present geometric features in relief—to the hydrazine-treated gels.³⁴ We employed fluorescently labeled protein to demonstrate uniform protein coating with no sign of enhanced border deposition, for both soft and stiff substrates (Figure S1). After seeding cells on these surfaces, we confirmed that single cells can be confined in small patterns ranging from 1000–20 000 μm^2 and multiple cells can exist in larger sized patterns

ranging from 5000–400 000 μm^2 area. Laser scanning confocal microscopy of patterned cells shows that cell height is higher in soft gels than stiff gels, decreases with increasing area and is higher for multicellular patterns than patterns with single cells (Figures S2 and S3). Morphological analysis reveals the average area of cells on stiff substrates is comparable to the pattern size (Figure S3). Patterned cells remained viable and restricted to the islands adhesive area for approximately 10 days in culture.

3.2. Influence of Single Cell Area and Geometry on MSC Phenotype. To examine the phenotype of patterned MSCs in response to hydrogel stiffness (0.5 and 30 kPa) and shape (different sizes and geometries), we studied the expression of the canonical MSC multipotency surface markers Endoglin and Stro-1 (Figure 1b–d).^{32,35} Constraining single cells to small islands leads to quiescence.³² Cells cultured on soft substrates show higher expression of multipotency markers compared to stiff substrates (~ 3 -fold higher for Endoglin and ~ 2 -fold higher for Stro-1). In addition, cells cultured in smaller islands (1000 μm^2) tend to express elevated MSC markers compared to cells cultured in large islands (20,000 μm^2) (~ 16.9 -fold (soft) and ~ 4.4 -fold (stiff) higher for Endoglin and ~ 5.9 -fold (soft) and ~ 3.8 -fold (stiff) higher for Stro-1). MSCs cultured on soft matrices showed higher expression of

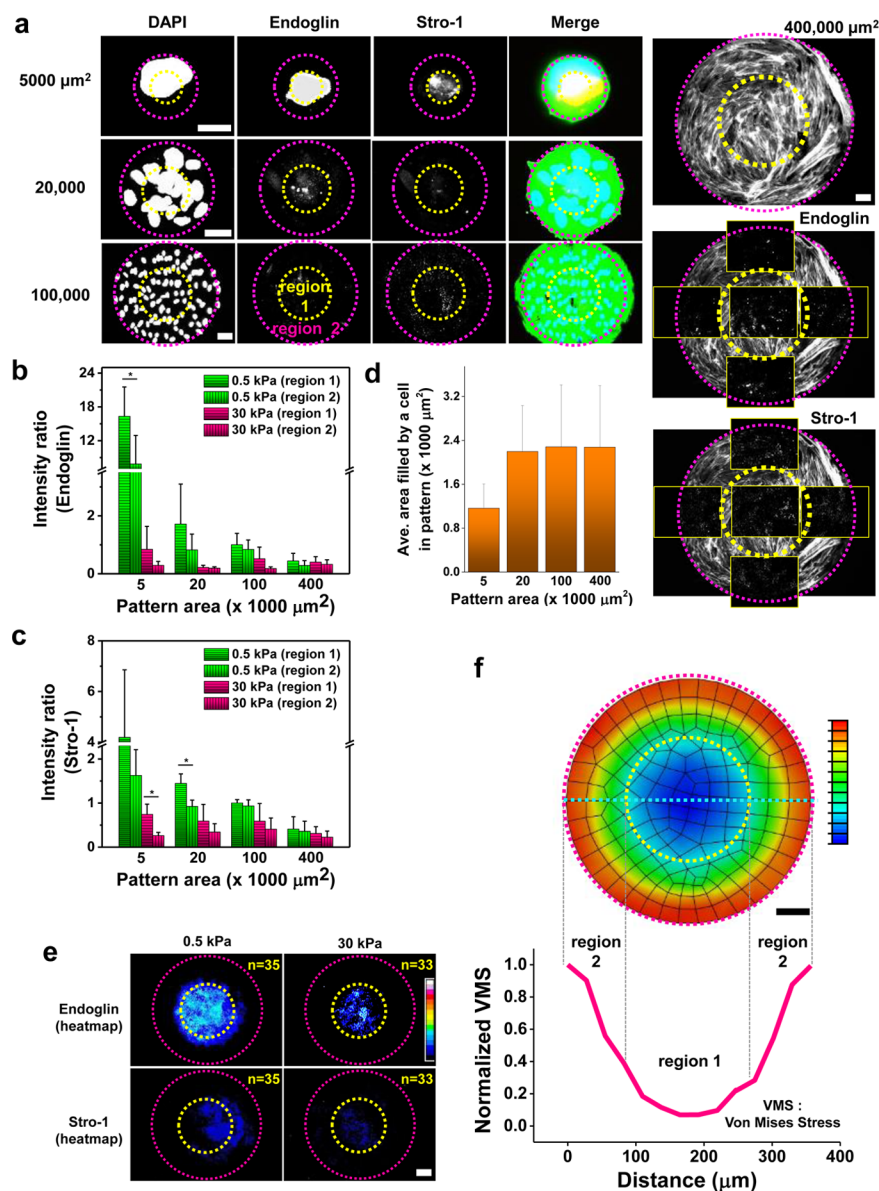


Figure 4. Geometry guides the spatial distribution of multipotency in multicellular patterns. (a) Representative immunofluorescence microscope images of multiple cells cultured in various sized circle patterns (5000 , $20\,000$, $100\,000$, and $400\,000\ \mu\text{m}^2$); dashed lines represent region 1 (interior) and region 2 (exterior). Quantitation of (b) Endoglin and (c) Stro-1 markers for patterned multiple cells divided by two different regions (cultured on soft ($0.5\ \text{kPa}$) and stiff ($30\ \text{kPa}$) substrates). (d) Average area filled by a cell cultured for 10 days in each sized pattern. (e) Representative immunofluorescence heatmaps of multiple cells stained for Endoglin and Stro-1 cultured in $100\,000\ \mu\text{m}^2$ size patterns for 10 days. (f) Representative modeled mechanical stress distribution of multicellular sheet of cells contracting on a $100\,000\ \mu\text{m}^2$ sized pattern and normalized von mises stress (VMS) across the patterns. Scale bar: $40\ \mu\text{m}$. ($N = 4$). ($*P < 0.05$, one-way ANOVA).

multipotency markers compared to those cultured on stiff substrates throughout the experiments (Figure S4). Because subcellular geometric cues have been shown to influence lineage specification,^{27,29} we tested various shapes of the same area ($3000\ \mu\text{m}^2$) (Figure 2a and b). We cultured MSCs in these patterns for 10 days, and found that cells on circular patterns showed higher levels of MSC markers relative to other shapes. Interestingly, regardless of stiffness, cells cultured in ovals (8:1 aspect ratio) showed the lowest levels of Endoglin expression compared to circular shapes (9.4-fold (soft) and 5.3-fold (stiff)), whereas Stro-1 marker expression was the lowest for cells in star shapes compared to circle shapes (11.6-fold (soft) and 21.7-fold (stiff)) (Figure 2c, d). The distribution of single cells that express MSC markers was also analyzed and

demonstrates that both substrate stiffness and size dependence (for single cells) influence the retention of the MSC phenotype (Figure S5). In addition, flow cytometry for endoglin and Stro-1 expression in MSCs cultured on TCP and on patterned and nonpatterned hydrogels of 0.5 and $30\ \text{kPa}$ were performed (Figure S6). While the differences in Endoglin expression were not significant across conditions as determined by flow, soft hydrogels promoted maintenance of Stro-1 expression for 10 days at levels comparable to cells freshly seeded from cryopreservation.

3.3. Influence of Cell Density on MSC Phenotype.

Although cells in vivo integrate and respond to various biophysical cues present in their microenvironments such as matrix stiffness and cell shape, cells are also often in contact

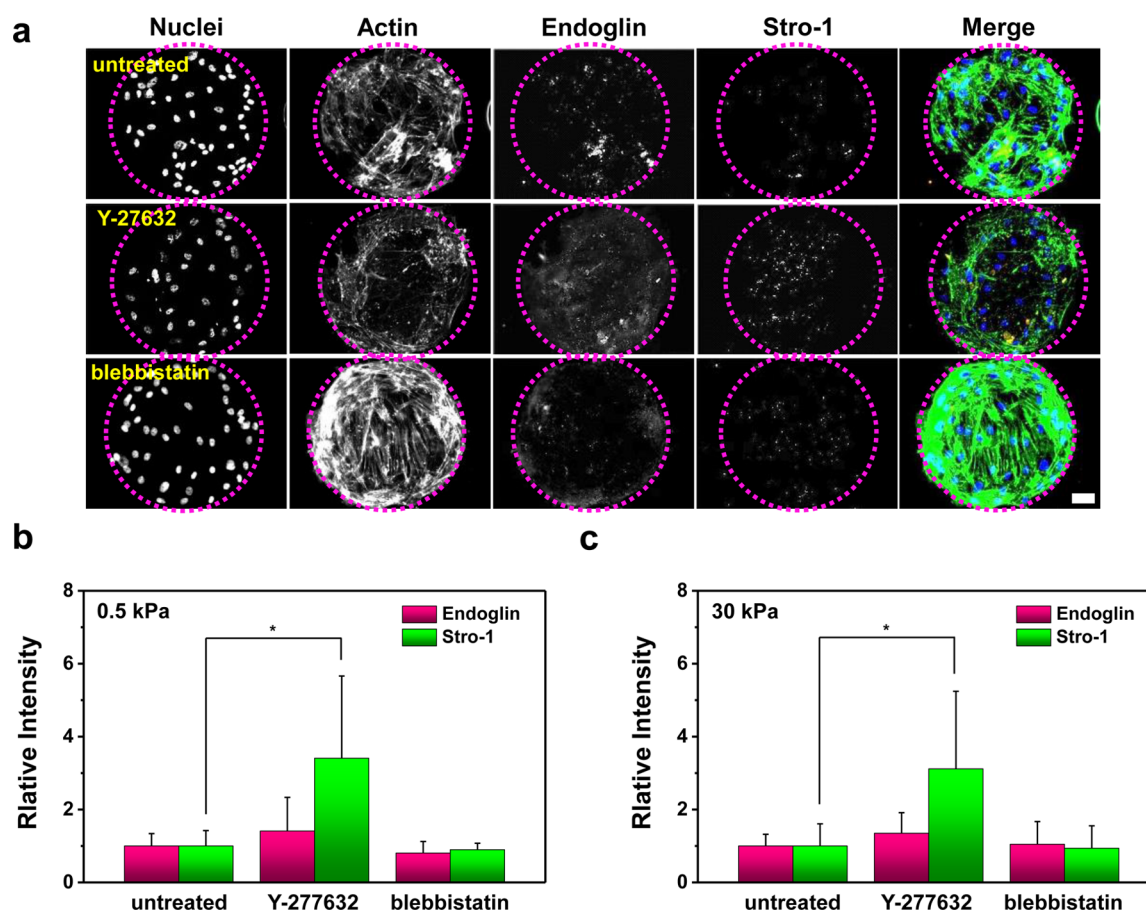


Figure 5. MSCs treated with actomyosin contractility inhibitors show elevated levels of multipotency markers. (a) Representative immunofluorescence microscope images of MSCs (0.5 kPa) stained for Endoglin and Stro-1 cultured with or without drug treatment (Scale bar: 40 μm). Expression of Endoglin and Stro-1 markers for cells cultured on (b) soft and (c) stiff substrates with and without drug treatment. ($N = 3$). (* $P < 0.05$, one-way ANOVA).

with neighboring cells. This contact may change how cells respond to these cues. Thus, we next investigated the effects of patterning multiple cells in large patterns on MSC phenotype. We employed circular patterns of 100 000 μm^2 and cultured cells for 10 days. Analogous to our single cell results, multiple cells cultured on soft substrates had higher expression of MSC markers compared to those cultured on stiff substrates. Islands with higher cell density showed increased expression of MSC markers (Figure 3a). Cells on soft substrates showed higher expression of MSC markers as cell number increased compared to those on stiff substrates (Figure 3b). The average number of cells per pattern was ~ 40 cells with a range from 1 to ~ 120 cells in the 100 000 μm^2 area of each pattern. Since seeding density was fixed, variations are likely due to irregular cell deposition after seeding. We also confirmed the effect of cell density on the maintenance of MSC multipotency marker expression by using square shapes (Figure S7), and we saw good correspondence with the results from the circular shapes. From confocal microscopy analysis, we confirmed that the results are not artifacts of cell density or debris (Figure 3c and Figure S8). We also examined the proliferation of MSCs in large circular patterns (100 000 μm^2) by culturing MSCs in 5-bromo-2'-deoxyuridine (BrdU) labeling reagent-containing media for 24 h at similar densities. At that time point, $\sim 22\%$ (soft) and $\sim 26\%$ (stiff) of cells cultured in patterns stained positive for BrdU (Figure S9). We found that the number of cells confined within a pattern—which influences the degree to

which they can spread—was correlated to the expression of MSC markers. For patterns on soft substrates (0.5 kPa), as the number of cells increase within a pattern, the spread area decreases (Figure S10) with an associated increase in the expression of MSC markers (Figure 4b). This observation is consistent with our studies of constraining single cell area (Figure 1). Furthermore, we compared large patterned cells to nonpatterned cells with similar density. Cells residing in central locations of very large patterns (400 000 μm^2) showed similar intensities to nonpatterned cells of similar density (Figure 4b and c). However, as pattern size decreases to ~ 100 000 μm^2 , cell organization and packing are more homogeneous compared to the elongated spread cells observed on nonpatterned substrates. To demonstrate this, we cultured MSCs for 10 days on 100 000 μm^2 circles or nonpatterned surfaces where cell density was the same. The results show that MSC marker expression is higher in patterned regions than nonpatterned regions (Figure S11).

Because an early report demonstrated how different regions of stress imposed on a population of patterned MSCs would guide differentiation,³⁰ we next investigated whether position within the pattern affected MSC state. To compare the MSC phenotype in different regions of circular patterns (5000, 20 000, 100 000, and 400 000 μm^2 , with an average of ~ 5 , 12, 48, and 175 cells per pattern, respectively), we superimposed a circle of half radius to divide the patterns into two regions (Figure 4a). Cells in region 1 (central region) show ~ 2 -fold

increase in Endoglin and Stro-1 expression compared to those in region 2 (outer region) (Figure 4b, c). In addition, cells in smaller sized patterns display higher levels of MSC marker expression. The average cell area when cultured in $5000 \mu\text{m}^2$ was ~ 2 -fold smaller than larger sized patterns ($20\,000$, $100\,000$, and $400\,000 \mu\text{m}^2$) (Figure 4d). MSCs cultured on soft substrates showed a less pronounced intensity difference between the two regions compared to stiff substrates (Figure S12). To further verify the influence of pattern region, we generated immunofluorescence heatmaps from both stains (Endoglin and Stro-1) via averaging the intensity of multiple overlaid immunofluorescence images using ImageJ (Figure 4e). Heatmaps showed cells on soft substrates maintain higher levels of multipotency compared to those on stiff substrates and that highest expression is localized to the central regions. We used finite element modeling of mechanical stress distributions in circular patterns and found that, for a connected layer, mechanical stress decreases closer to the center regions, which corresponds with the results of the experiments (Figure 4f).

Taken together, our results demonstrate a clear influence of substrate stiffness, cell shape and position in multicellular architectures on maintaining the expression of multipotency markers. However, we acknowledge that some variability in cell division (self-renewal or differentiation) across the substrates may affect the multipotent outcome.

3.4. Role of Cytoskeletal Tension in Maintaining MSC Phenotype. From the results of multicellular studies in circular patterns, mechanical stress will influence the expression of MSC markers. To explore whether the stress from the patterns influences the MSC phenotype through cytoskeletal tension, we treated cells with Y-27632 (an inhibitor of rho-associated kinases) and blebbistatin (an inhibitor of myosin II). MSCs were cultured in $100\,000 \mu\text{m}^2$ circular geometries with or without 2 mM Y-27632 or 1 mM blebbistatin for 10 days. Cells cultured with Y-27632 show increased expression of both Endoglin and Stro-1, which reveals that restriction of cytoskeletal tension plays a significant role. However, treatment with blebbistatin did not influence expression levels (Figure 5). In terms of cell spreading, untreated and blebbistatin treated cells were similar but Y-27632 treated cells displayed lower spreading. The degree of cell spreading with Y-27632 treatment was less than untreated cells, resulting in higher levels of multipotency markers. Because the seeding density of cells was fixed, we could indirectly compare the proliferation rates between untreated and drug treated cells. Average cell densities were similar suggesting that drug treatment at the tested concentration makes little difference in proliferation rates. In addition, cells on stiff substrates express lower levels of multipotency markers compared to those on soft substrates (Figure S13).

4. DISCUSSION

Within the stem cell niche, cells are exposed to various combinations of biochemical and biophysical factors. MSC fate decisions are influenced by the properties of the niche, which provide a highly specialized microenvironment for maintenance of the multipotent phenotype and for lineage specification. Recently, Yang et al.³⁶ and Lee et al.¹⁵ demonstrated how MSCs cultured on stiff materials can “remember” their environment, which may limit their potential to differentiate to softer lineages. Understanding how biophysical cues influence the MSC phenotype and controlling these aspects

ex vivo will be critical for leveraging the broad therapeutic potential of MSCs.

Previously, we had shown that restricting cell spreading using micropatterned islands on rigid materials leads to maintenance of the multipotent phenotype and prevention of inappropriate lineage specification.³² Because the degree of cell spreading—by microconfinement or through control of substrate stiffness—has been shown to modulate cytoskeletal tension and MSC fate decisions,^{37–40} we fixed the adhesion area of the cells while tuning the stiffness of the substrate. Single MSCs captured in circular shapes show elevated expression of multipotency markers compared to those cultured on non-patterned gels. This expression decreases as the cell adhesive area is increased. This trend in MSC marker expression holds for both soft and stiff substrates; however, in all cases, MSCs adherent to soft hydrogels display higher MSC marker expression levels. This finding is consistent with our work with microconfined MSCs on rigid materials³² and suggests that soft materials—previously demonstrated to influence MSC quiescence¹⁴—may also serve to retain multipotency. Interestingly, the expression of multipotency markers for cells cultured in $1000 \mu\text{m}^2$ features on stiff substrates is similar to the level of that for cells cultured in $5000 \mu\text{m}^2$ patterns on soft substrates. This result demonstrates how MSC multipotency may be influenced by combinations of the interrelated biophysical parameters stiffness and cell size (the degree of spreading). This led us to ask whether controlling subtle geometric features in cells of the same total adhesive area may have an influence on the MSC phenotype. We micropatterned single cells in various geometries with a constant adhesive area ($3000 \mu\text{m}^2$). Shapes that foster high degrees of cytoskeletal stress such as stars and ovals of different aspect ratios¹² showed lower expression levels of MSC markers over time compared to circular shapes. This result suggests that, in addition to spreading, discrete geometric cues at the perimeter of single cells will promote the loss of the multipotent phenotype. Certain shapes appeared to differentially modulate different markers. For instance, MSCs in the elongated oval shape led to the largest decrease in Endoglin expression, while star shaped cells showed the largest decrease in Stro-1. Both of these shapes have been shown previously to enhance osteogenesis in single MSCs.¹² Exploring differences between these shapes in regulating multipotency (and differentiation) is outside of the scope of this study. Nevertheless, it demonstrates how micropatterning platforms may be used in future work to explore subtle mechanobiology phenomena.

In addition to single cells, geometric features at the multicellular level have been demonstrated to modulate cell behavior ranging from growth control to differentiation.^{30,31} For example, Ruiz et al. demonstrated how MSC aggregates grown on outer regions, which show high local strains, tend to differentiate into the osteogenic lineage while those cultured at inner regions, which display low cytoskeletal tension, prefer to differentiate into the adipocyte lineage when cultured with mixed induction media.³⁰ Inspired by this study, and our observations that significant numbers of MSCs in culture on these materials remain multipotent, we hypothesized that MSCs cultured in multicellular arrangements would show patterns of multipotency marker expression. Patterns with a higher density of cells (which restricts spreading) led to higher expression of multipotency markers compared to patterns with a lower density of cells (which promotes spreading). To investigate how mechanical stress fostered by multicellular

geometries may influence MSC multipotency, we explored circular patterns of various areas (5000–400 000 μm^2) and examined two different regions within each pattern (perimeter and interior). MSC marker expression decreased in cells that were cultured near the perimeter region while cells in the pattern interior showed the highest levels of expression. This trend in regional expression of MSC markers is observed on both soft and stiff substrates, but with enhanced expression seen on the softer materials. Using a finite element model of cellular sheet contraction, we see that the perimeter region promotes the highest degree of stress. This model is based on interconnected nodes and its results would only apply where there is force transmission between cells in multicellular aggregates, through cell–cell interaction. Cadherin junctions have been implicated in 3D MSC aggregation⁴¹ and, although this is a 2D system, there may be an aggregating effect due to patterning the cells. Further investigation is needed to determine whether such interactions are present or are promoted in this system. Note that patterning influences the degree in which cells can spread initially and leads to the development of two types of cells within the geometric confinement: (1) cells experiencing a high degree of stress at the perimeter, and (2) tightly packed cells in the interior. Therefore, the large patterns separated the cells into two distinct regions with different patterns of marker expression.

To further verify the importance of low cytoskeletal tension in maintaining MSC phenotype, we used inhibitors of actomyosin contractility on our patterned cultures. Cells were treated with the Rho-associated protein kinase inhibitor (ROCK) Y-27632 and the nonmuscle myosin inhibitor blebbistatin. Inhibiting cytoskeletal tension after cell adhesion using pharmacological inhibitors promotes higher expression of MSC markers, particularly when targeting ROCK. This suggests that signaling through Rho-kinase may play a role in regulating the multipotent phenotype, which is consistent with the role of ROCK during MSC differentiation.^{27,38}

5. CONCLUSIONS

In this work, we explored the combined influence of matrix elasticity and cell/tissue geometry on regulating the MSC phenotype. Conditions that foster a low state of cytoskeletal tension—either through control of substrate stiffness, restricting spreading via high cell density, or through micropatterning single cells or constraining populations of cells in defined multicellular islands—will maintain the expression of MSC multipotency markers compared to cells grown on tissue culture plastic ware. From finite element models and the results of our immunofluorescence experiments, we see that interior regions of large populations of cells foster a low degree of tension, which promotes maintenance of the MSC phenotype. This work shows how multiple biophysical parameters on cell culture materials can be tuned alone and in parallel to maintain the MSC phenotype, to guide our understanding of the MSC microenvironment, and assist the selection of appropriate cell culture materials for regenerative therapies.

■ ASSOCIATED CONTENT

Supporting Information

The following file is available free of charge on the ACS Publications website at DOI: 10.1021/ab500003s.

Data of MSC multipotency over culture time, flow cytometry, BrdU marker expression, fluorescence images of patterned adhesion ligands ([PDF](#))

■ AUTHOR INFORMATION

Corresponding Author

*E-mail: kakilian@illinois.edu.

Notes

The authors declare no competing financial interest.

■ ACKNOWLEDGMENTS

This work was supported by the National Heart Lung and Blood Institute of the National Institutes of Health, Grant 11323188.

■ REFERENCES

- (1) Li, L.; Xie, T. Stem cell niche: structure and function. *Annu. Rev. Cell Dev. Biol.* **2005**, *21*, 605–631.
- (2) Scadden, D. T. The stem-cell niche as an entity of action. *Nature* **2006**, *441*, 1075–1079.
- (3) Jones, D. L.; Wagers, A. J. No place like home: anatomy and function of the stem cell niche. *Nat. Rev. Mol. Cell Biol.* **2008**, *9*, 11–21.
- (4) Da Silva Meirelles, L.; Chagastelles, P. C.; Nardi, N. B. Mesenchymal stem cells reside in virtually all post-natal organs and tissues. *J. Cell Sci.* **2006**, *119*, 2204–2213.
- (5) Crisan, M.; Yap, S.; Casteilla, L.; Chen, C.-W.; Corselli, M.; Park, T. S.; Andriolo, G.; Sun, B.; Zheng, B.; Zhang, L.; et al. A perivascular origin for mesenchymal stem cells in multiple human organs. *Cell Stem Cell* **2008**, *3*, 301–313.
- (6) Kilian, K. A.; Mrksich, M. Directing stem cell fate by controlling the affinity and density of ligand-receptor interactions at the biomaterials interface. *Angew. Chem., Int. Ed. Engl.* **2012**, *51*, 4891–4895.
- (7) Hennrick, K. T.; Keeton, A. G.; Nanua, S.; Kijek, T. G.; Goldsmith, A. M.; Sajjan, U. S.; Bentley, J. K.; Lama, V. N.; Moore, B. B.; Schumacher, R. E.; et al. Lung cells from neonates show a mesenchymal stem cell phenotype. *Am. J. Respir. Crit. Care Med.* **2007**, *175*, 1158–1164.
- (8) Keating, A. Mesenchymal stromal cells: new directions. *Cell Stem Cell* **2012**, *10*, 709–716.
- (9) Engler, A. J.; Sen, S.; Sweeney, H. L.; Discher, D. E. Matrix elasticity directs stem cell lineage specification. *Cell* **2006**, *126*, 677–689.
- (10) Rowlands, A. S.; George, P. A.; Cooper-White, J. J. Directing osteogenic and myogenic differentiation of MSCs: interplay of stiffness and adhesive ligand presentation. *Am. J. Physiol.* **2008**, *295*, C1037–C1044.
- (11) Tse, J. R.; Engler, A. J. Stiffness gradients mimicking in vivo tissue variation regulate mesenchymal stem cell fate. *PLoS One* **2011**, *6*, e15978.
- (12) Lee, J.; Abdeen, A. A.; Huang, T. H.; Kilian, K. A. Controlling cell geometry on substrates of variable stiffness can tune the degree of osteogenesis in human mesenchymal stem cells. *J. Mech. Behav. Biomed. Mater.* **2014**, *38*, 209–218.
- (13) Abdeen, A. A.; Weiss, J. B.; Lee, J.; Kilian, K. A. Matrix Composition and Mechanics Direct Proangiogenic Signaling from Mesenchymal Stem Cells. *Tissue Eng., Part A* **2014**, *20*, 2737–2745.
- (14) Winer, J. P.; Janmey, P. A.; McCormick, M. E.; Funaki, M. Bone marrow-derived human mesenchymal stem cells become quiescent on soft substrates but remain responsive to chemical or mechanical stimuli. *Tissue Eng., Part A* **2009**, *15*, 147–154.
- (15) Lee, J.; Abdeen, A. A.; Kilian, K. A. Rewiring mesenchymal stem cell lineage specification by switching the biophysical microenvironment. *Sci. Rep.* **2014**, *4*, 5188.

- (16) Khalil, A. S.; Xie, A. W.; Murphy, W. L. Context clues: the importance of stem cell-material interactions. *ACS Chem. Biol.* **2014**, *9*, 45–56.
- (17) Murphy, W. L.; Mcdevitt, T. C.; Engler, A. J. Materials as stem cell regulators. *Nat. Mater.* **2014**, *13*, 547–557.
- (18) Higuchi, A.; Ling, Q.; Chang, Y.; Hsu, S.; Umezawa, A. Physical Cues of Biomaterials Guide Stem Cell Differentiation Fate. *Chem. Rev.* **2013**, *113*, 3297–3328.
- (19) Guilak, F.; Cohen, D. M.; Estes, B. T.; Gimble, J. M.; Liedtke, W.; Chen, C. S. Control of stem cell fate by physical interactions with the extracellular matrix. *Cell Stem Cell* **2009**, *5*, 17–26.
- (20) Ghaemi, S. R.; Harding, F. J.; Delalat, B.; Gronthos, S.; Voelcker, N. H. Exploring the mesenchymal stem cell niche using high throughput screening. *Biomaterials* **2013**, *34*, 7601–7615.
- (21) Gilbert, P. M.; Havenstrite, K. L.; Magnusson, K. E. G.; Sacco, A.; Leonardi, N. A.; Kraft, P.; Nguyen, N. K.; Thrun, S.; Lutolf, M. P.; Blau, H. M. Substrate elasticity regulates skeletal muscle stem cell self-renewal in culture. *Science* **2010**, *329*, 1078–1081.
- (22) Skardal, A.; Mack, D.; Atala, A.; Soker, S. Substrate elasticity controls cell proliferation, surface marker expression and motile phenotype in amniotic fluid-derived stem cells. *J. Mech. Behav. Biomed. Mater.* **2013**, *17*, 307–316.
- (23) Oh, S.; Brammer, K. S.; Li, Y. S. J.; Teng, D.; Engler, A. J.; Chien, S.; Jin, S. Stem cell fate dictated solely by altered nanotube dimension. *Proc. Natl. Acad. Sci. U.S.A.* **2009**, *106*, 2130–2135.
- (24) Park, J.; Bauer, S.; von der Mark, K.; Schmuki, P. Nanosize and vitality: TiO₂ nanotube diameter directs cell fate. *Nano Lett.* **2007**, *7*, 1686–1691.
- (25) McMurray, R. J.; Gadegaard, N.; Tsimbouri, P. M.; Burgess, K. V.; McNamara, L. E.; Tare, R.; Murawski, K.; Kingham, E.; Oreffo, R. O. C.; Dalby, M. J. Nanoscale surfaces for the long-term maintenance of mesenchymal stem cell phenotype and multipotency. *Nat. Mater.* **2011**, *10*, 637–644.
- (26) Chen, C. S.; Mrksich, M.; Huang, S.; Whitesides, G. M.; Ingber, D. E. Geometric control of cell life and death. *Science* **1997**, *276*, 1425–1428.
- (27) Kilian, K. A.; Bugarija, B.; Lahn, B. T.; Mrksich, M. Geometric cues for directing the differentiation of mesenchymal stem cells. *Proc. Natl. Acad. Sci. U.S.A.* **2010**, *107*, 4872–4877.
- (28) Fu, J.; Wang, Y. K.; Yang, M. T.; Desai, R. A.; Yu, X.; Liu, Z.; Chen, C. S. Mechanical regulation of cell function with geometrically modulated elastomeric substrates. *Nat. Methods* **2010**, *7*, 733–736.
- (29) Lee, J.; Abdeen, A. A.; Zhang, D.; Kilian, K. A. Directing stem cell fate on hydrogel substrates by controlling cell geometry, matrix mechanics and adhesion ligand composition. *Biomaterials* **2013**, *34*, 8140–8148.
- (30) Ruiz, S. A.; Chen, C. S. Emergence of patterned stem cell differentiation within multicellular structures. *Stem Cells* **2008**, *26*, 2921–2927.
- (31) Nelson, C. M.; Jean, R. P.; Tan, J. L.; Liu, W. F.; Sniadecki, N. J.; Spector, A. A.; Chen, C. S. Emergent patterns of growth controlled by multicellular form and mechanics. *Proc. Natl. Acad. Sci. U.S.A.* **2005**, *102*, 11594–11599.
- (32) Zhang, D.; Kilian, K. A. Biomaterials The effect of mesenchymal stem cell shape on the maintenance of multipotency. *Biomaterials* **2013**, *34*, 3962–3969.
- (33) Tse, J. R.; Engler, A. J. Preparation of hydrogel substrates with tunable mechanical properties. *Curr. Protoc. Cell Biol.* **2010**, *47*, 10.16.1–10.16.16.
- (34) Damljanović, V.; Lagerholm, B. C.; Jacobson, K. Bulk and micropatterned conjugation of extracellular matrix proteins to characterized polyacrylamide substrates for cell mechanotransduction assays. *Biotechniques* **2005**, *39*, 847–851.
- (35) Dalby, M. J.; Gadegaard, N.; Tare, R.; Andar, A.; Riehle, M. O.; Herzyk, P.; Wilkinson, C. D. W.; Oreffo, R. O. C. The control of human mesenchymal cell differentiation using nanoscale symmetry and disorder. *Nat. Mater.* **2007**, *6*, 997–1003.
- (36) Yang, C.; Tibbitt, M. W.; Basta, L.; Anseth, K. S. Mechanical memory and dosing influence stem cell fate. *Nat. Mater.* **2014**, *13*, 645–652.
- (37) Re, F.; Zanetti, A.; Sironi, M.; Polentarutti, N.; Lanfrancone, L.; Dejana, E.; Colotta, F. Inhibition of anchorage-dependent cell spreading triggers apoptosis in cultured human endothelial cells. *J. Cell Biol.* **1994**, *127*, 537–546.
- (38) McBeath, R.; Pirone, D. M.; Nelson, C. M.; Bhadriraju, K.; Chen, C. S. Cell shape, cytoskeletal tension, and RhoA regulate stem cell lineage commitment. *Dev. Cell* **2004**, *6*, 483–495.
- (39) Khetan, S.; Guvendiren, M.; Legant, W. R.; Cohen, D. M.; Chen, C. S.; Burdick, J. A. Degradation-mediated cellular traction directs stem cell fate in covalently crosslinked three-dimensional hydrogels. *Nat. Mater.* **2013**, *12*, 1–8.
- (40) Guvendiren, M.; Burdick, J. A. Stiffening hydrogels to probe short- and long-term cellular responses to dynamic mechanics. *Nat. Commun.* **2012**, *3*, 792.
- (41) Sart, S.; Tsai, A. C.; Li, Y.; Ma, T. Three-Dimensional Aggregates of Mesenchymal Stem Cells. *Tissue Eng., Part B* **2014**, *20*, 365–380.